AWESOME

WATER-ECOSYSTEM-FOOD

MESO LEVEL MODEL

October, 2022

This project is part of the PRIMA Programme supported by the European Union, having received funding from it under grant agreement No 1942

Programme Call:	PRIMA Call 2019 Section 1 Farming RIA
Project Number:	1942
Project Title:	AWESOME
Partners:	POLIMI (Project Coordinator), AUEB, YVC, UH, AF, RWTH, FEEM
Work-Package:	WP4
Deliverable #:	D4.2
Deliverable Type:	Document
Contractual Date of Delivery:	31 October 2022
Actual Date of Delivery:	28 October 2022
Title of Document:	Meso level model
Author(s):	Elena Matta, Veronica Piuri, Matteo Giuliani, Guang Yang, and Andrea Castelletti
Content of this report:	Report describing the meso level simulation model and its interactions with the macro and micro levels. The report will also include the analysis of the performance of candidate portfolios under current water availability and demands.
Availability:	This report is public.

Document revisions		
Author	*Revision content*	*Date*
Elena Matta, Veronica Piuri	D4.2_v01 – First draft of the report	28 Sep. 2022
Veronica Piuri, Matteo Giuliani	D4.2_v02 – revised version with new results	29 Sept. 2022
Ricarda Lothmann, Julia Sirota	Internal revision	11 Oct. 2022
Matteo Giuliani, Veronica Piuri, Elena Matta	D4.2_v03 – revised version (final)	27 Oct. 2022
Andrea Castelletti, Elena Matta	Final check and submission	28 Oct. 2022

Table of Content

LIST OF ACRONYMS

Abbreviations

ANN:	Artificial Neural Network
HAD:	High Aswan Dam
CS:	Case Study
D:	Deliverable
DAF:	Decision Analytic Framework
DM:	Decision Maker
DoA:	Description of Action
EMODPS:	Evolutionary multi-objective direct policy search
ES:	Ecosystem Services
GA:	Grant Agreement
GERD:	Grand Ethiopian Renaissance Dam
MAWGs:	Multi-Actor Working Groups
MER:	Merowe Dam
MOEA:	Multi-objective evolutionary optimization algorithm
MS:	Milestone
NRB:	Nile River Basin
PIP:	Participatory and Integrated Planning
POLIMI:	Politecnico di Milano
RBS:	Radial Basis Function
RO:	Reverse Osmosis
SH:	Stakeholder
T:	Task
WEFE-Nexus:	Water Energy Food Ecosystem-Nexus
WP:	Work Package

EXECUTIVE SUMMARY

Deliverable 4.2 describes the strategic model at the meso level and its interactions with the macro and micro levels, including its methodological components. It also reports the simulations of existing water availability and water distribution systems, accounting for the water, energy, food and ecosystem synergies and trade-offs. The document includes the analysis of some candidate planning portfolios - in terms of water supply and water demand - and their associated performance as quantified by the evaluation indicators formulated in D4.1. Key findings about the water supply model indicate a clear trade-off between hydropower production and irrigation abstraction in Sudan. In addition, the considered portfolios do not show substantial conflicts between irrigation in Egypt and Sudan. As for the water demand, the portfolios analyzed in this report show that the introduction of advanced water demand technologies such as aquaponics and desalination can reduce water demands, but they require high initial investments. Similar water demand reductions can be obtained at lower costs by increasing water reuse and groundwater pumping, but this strategy has high environmental risks.

1. INTRODUCTION

Deliverable D4.2 (Meso level model) is the report describing the strategic model at the meso level and how it interacts with the other project levels (micro and macro). The document builds on the previous Milestone report MS14 (Decision analytic platform architecture) and further develops it. The work is an outcome of WP4 – specifically, of Task T4.2, in which the main objective is developing a strategic model running at the meso scale to simulate the existing water availability and water distribution system and accounting for the water, food, and energy demands as well as significant regional policies and ecosystem services (WEFE nexus). The model is being used to map the candidate portfolios identified in Task T4.1 into their associated performance as quantified by the evaluation indicators (s. Deliverable D4.1 Candidate portfolios and evaluation indicators for WEF Nexus analysis).
The broader goal of WP4 is to develop a Decision-Analytic Framework (DAF) running at the river basin scale. It relies on a detailed characterization of different innovative technological solutions demonstrated in WP5 at the micro-level (e.g., aquaponics) and a realistic representation of macro-scale processes and regional policies influencing river basin dynamics in terms of land use, water and energy supply, and ecosystem services (WP2, WP3). Besides, the case study assessments and participatory processes initiated by WP6 support our activities, integrating stakeholders (SHs) views and interests to shape our analyses. The combination of systems analysis methods and advanced a-posteriori multi-objective evolutionary optimization algorithms (MOEAs) allows the discovery of a set of efficient solutions and associated performance with respect to the WEFE multi-dimensional assessment space, where SHs and policy-makers are able to explore multi-sectoral trade-offs and negotiate potential compromise alternatives. The workflow of WP4 and its interconnections with the other WPs are illustrated in Figure 1.

The DAF employs a strategic river model coupled with an optimization engine: the river model is a parsimonious model conceptualising the main natural processes and human decisions at the whole river basin scale. The optimization engine implements a simulation-based optimization via multi-objective evolutionary algorithms [1], which iteratively improves a set of candidate solutions in terms of their performance estimated via simulation of the strategic model at the meso level with respect to the selected evaluation indicators (s. Figure 2). In this deliverable, some candidate portfolios are evaluated via simulation of the strategic model to assess their performance as quantified by the evaluation indicators. In Task T4.3, we will instead use the optimization engine to obtain efficient portfolios and better capture synergies and trade-offs across the WEFE Nexus.

The report is structured as follows: the next section describes the general decision analytic framework in all its methodological components (e.g., water system model, optimisation engine), Section 3 presents the strategic model of the Nile River Basin (NRB), while Section 4 reports the analysis and evaluation of the selected planning portfolios, in terms of water demand and water supply.

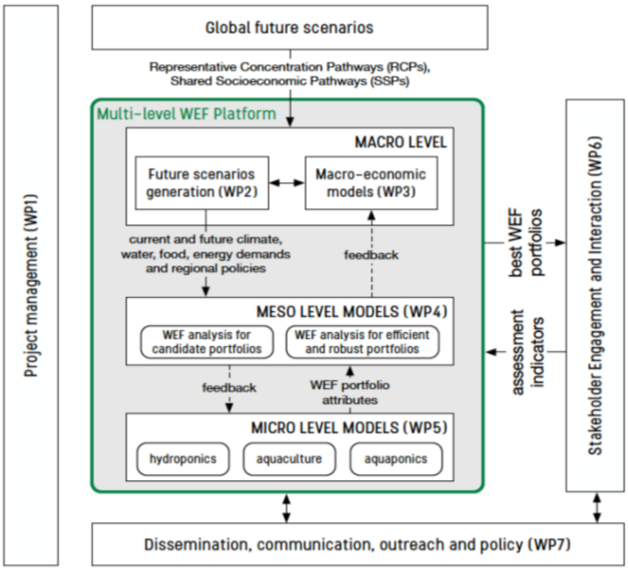

Figure 1– AWESOME project structure.

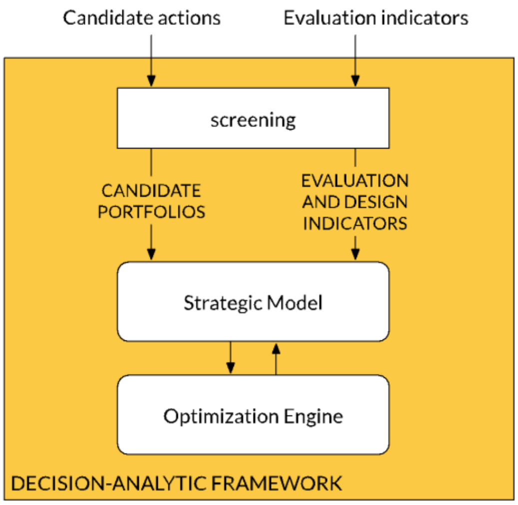

Figure 2 – Strategic DAF model at the meso level.

2. DECISION ANALYTIC FRAMEWORK

In this section, all the elements of a generic strategic (or design) model developed for an illustrative, hypothetical water system are described. The same model components are then combined into the strategic meso level model of the NRB, described in detail in Section 3 of this report.

2.1 STRATEGIC WATER SYSTEM MODEL

The main elements of the model are presented considering the illustrative system represented in Figure 3. As can be observed, there are four main system components: a water reservoir, the associated hydropower plant, an irrigation district downstream the reservoir, and an environmentally vulnerable river stretch downstream the reservoir and the irrigation district.
The reservoir dynamics is described by the mass balance equation of the water volume s_t stored in the reservoir at the beginning of month t:

$$s_{t+1} = s_t + q_{t+1} - r_{t+1} \quad (1)$$

where q_{t+1} is the net inflow to the reservoir (i.e., inflow minus evaporation losses[i]) in the time interval $[t; t+1)$ and r_{t+1} the volume of water released in the same time interval. In the adopted notation, the time subscript of a variable indicates the time instant when its value is deterministically known. The storage s_t is observed at time t, whereas the inflow has subscript *t+1*, denoting the realization of the inflow stochastic process in the time interval [t,t+1).

The release is defined as $r_{t+1} = f(s_t, u_t, q_{t+1})$ where $f(\cdot)$ describes the nonlinear, stochastic relation between the release decision determined by the operating policy, i.e. $u_t = p(\cdot)$, and the actual release r_{t+1}, as in [2]. The actual release at the end of the time interval is generally equal to the release decision unless physical constraints prohibit it (e.g., if the prescribed release lies outside the minimum and maximum allowable releases, if there is insufficient water to meet the prescribed release, or if the prescribed release would result in the reservoir storage capacity being exceeded).

As for the irrigation district, it can abstract water from the river through a regulated water diversion channel. The diverted volume of water a_{t+1} is determined by the following hedging rule (adapted from [3]):

$$a_{t+1} = \begin{cases} \min\left(r_{t+1}, w_t^I(u^P) \cdot \left[\frac{r_{t+1}}{hdg}\right]^m\right) & if\ r_{t+1} \leq hdg \\ \min\left(r_{t+1}, w_t^I(u^P)\right) & otherwise \end{cases} \quad (2)$$

where r_{t+1} is the release from the reservoir, which corresponds to the water available in the river right upstream the irrigation district, $w_t^I(u^P)$ is the irrigation water demand that depends on the planning decision u^P (e.g., crop type, irrigation technique), whereas hdg and m are two parameters determining the operation of the irrigation diversion.

Downstream the irrigation diversion, the water volume left in the river $\varrho_{t+1} = r_{t+1} - a_{t+1}$ flows through an environmentally vulnerable river stretch providing valuable ecosystem services. In the model, all river reaches (black straight lines in Figure 3) are described using a simple plug-flow model

[i] This basic formulation of the mass balance equation can be refined for better representing the different water fluxes, such as evaporation, seepage, precipitation.

in which the velocity and direction of flow are assumed constant everywhere, without any lamination effect.

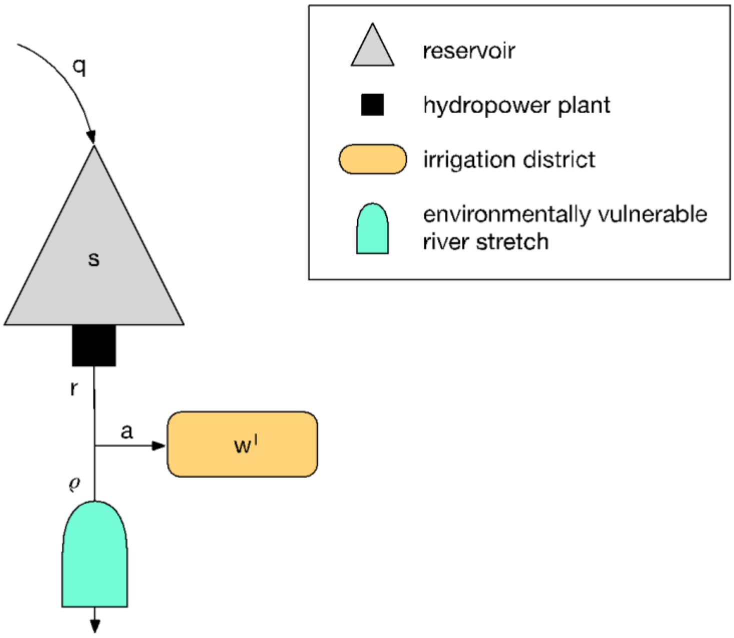

Figure 3 – Simplified topologic scheme displaying all the elements of the strategic simulation model.

2.2 EVALUATION AND DESIGN INDICATORS

Several stakeholders with conflicting interests (e.g., hydropower production vs irrigation deficit vs environmental flow deficit) may be affected by the reservoir and irrigation system operations. In the AWESOME project, these conflicting interests are captured by a set of evaluation indicators, which have been introduced in D4.1. A subset of these evaluation indicators will be then selected to represent the WEFE design indicators (or operating objectives) $J = |J^1, \dots, J^K|$ for the DAF optimization in Task T4.3.

Considering the illustrative example in Figure 3, three main components of the nexus (i.e., water-ecosystem, energy, and food) are affected by the operations of the system. Their conflicting interests can be thus modelled as follows[ii]:

- Environmental flow deficit (water):

[ii] It must be noted that the mathematical formulation of the three WEF operating objectives is purely illustrative, as it will be indeed adapted to the case study considered.

$$J^W = \frac{1}{H}\left[\sum_{t=0}^{H-1} \left(max\,(w_t^E - \underline{r}_{t+1}, 0)\right)\right] \quad (4)$$

where w_t^E is the specified environmental flow to be satisfied, and $\underline{r}_{t+1} = r_{t+1} - a_{t+1}$ is the amount of water entering the ecosystem sensitive area downstream of the irrigation abstraction (a_{t+1}).

- Annual hydropower production (energy):

$$J^E = \frac{1}{Nyears}\left[\sum_{t=0}^{H-1} P_{t+1}\right] \quad (5)$$

where P_{t+1} is the monthly hydropower production calculated as $P_{t+1} = \eta g \gamma \underline{h}_t q_{t+1}^{turb}$, where $\eta\ [-]$ is the turbines efficiency, $g = 9.81\ [m/s^2]$ is the gravitational acceleration, $\gamma = 1000\ [kg/m^3]$ is the water density, $\underline{h}_t\ [m]$ is the net hydraulic head, and $q_{t+1}^{turb}\ [m^3/s]$ is the turbinated flow.

- Squared irrigation deficit normalized with respect to squared irrigation demand (food):

$$J^F = \frac{1}{H}\left[\sum_{t=0}^{H-1} \left(\frac{max\,(w_t^I - a_{t+1}, 0)}{w_t^I}\right)^2\right] \quad (6)$$

where $w_t^I\ and\ a_{t+1}$ are the irrigation water demand and abstraction, respectively.

2.3 DECISION VARIABLES

Considering the illustrative example in Figure 3, two types of decisions including both the operation of the reservoir and the irrigation diversion (management actions) and farmers' decisions about crop types and/or irrigation techniques (planning actions) should be specified.

The management problem requires sequential decisions to be taken at discrete time instants. In the reservoir operation problem, the release decision u_t is determined at each time step by a closed-loop operating policy that depends on the current system conditions (e.g., time instant and reservoir storage), i.e. $u_t = p(t, s_t)$. In the irrigation abstraction problem, the decisions concern the water volume diverted into the irrigation channel, which is determined by the hedging rule formulated in Equation 2, which depends on the two time-invariant parameters hdg and m along with the water released from the reservoir.

On the other end, the planning problem requires to specify planning decisions u^P that are taken once, without considering how they might influence analogous decisions in the future. Note that the absence of dynamics in this type of decision does not imply, however, that also the system has to be non-dynamic.

2.4 OPTIMIZATION ENGINE

2.4.1 Optimization of system operation

The design problem of an optimal operating policy for water systems traditionally employed dynamic programming (DP) and its stochastic extension (i.e., stochastic dynamic programming -

SDP) [4,5]. SDP formulates the operating policy design problem as a sequential decision-making process, where a decision taken now produces an immediate reward, affects the next system state and, through that, all the subsequent rewards. The search for optimal policies employs value functions defined over a discrete (or discretized) state-decision space, which are obtained by looking ahead to future events and computing a backed-up value.

The decision u_t (see section 2.3 for details) is determined at each time step by an operating policy:

$$u_t = p(t, s_t) \quad (7)$$

and the state of the system is the reservoir storage s_t, which is altered according to the transition function described in Equation 1. The sequence of states over the time horizon defines a system trajectory, which allows the evaluation of the performance of the operating policy p by means of the objective function (i.e., design indicators defined in (3)). The optimal policy p^* is hence obtained by solving the following problem:

$$p^* = arg \min_p \boldsymbol{J} = |J^W, J^E, J^F| \qquad (8)$$

The DP-family methods solve this problem (8) by estimating the expected long-term cost of a policy for each state s_t, at time t by means of the value function, defined over a discrete grid of states and decisions:

$$H_t(s_t) = \Psi_{q_{t+1}} [\Phi_t(g_t(s_t, u_t, q_{t+1}),\ H_{t+1}(s_{t+1}))] \quad (9)$$

Where $H_t(\cdot)$ is the optimal cost-to-go function for a scalarized objective and $g_t(\cdot)$ is the corresponding scalarized immediate and time-separable cost function associated to the transition from state s_t to state s_{t+1} under the decision u_t. The modeling assumptions required by SDP for its application are finite domains of state, decision, and disturbance variables, time-separability of objective functions and constraints. These relatively mild assumptions imply, in theory, a wide applicability of SDP to many problems, but in practice its adoption is challenged by three curses (dimensionality, modeling, and multiple objectives) that considerably limit its use in real life complex problems [6].

Stochastic Dynamic Programming (SDP) has been considered, since the '60s [7,8], the best method to preserve a realistic problem structure due to mild requirements on systems representation [9], favoring its adoption in practical applications [10–12] and its systematic use in the reservoir operation literature [13–18]. Yet, SDP has several limitations that constrain problem framing in addressing emerging challenges in water system operations:

(a) the well-known curse of dimensionality [5] limits the dimension of the system to two or three reservoirs due to the exponential growth of computational cost with the number of state variables;

(b) the curse of modeling [19] requires all variables used as input in the operating policy to be described by a dynamic model, contributing additional state variables;

(c) the curse of multiple objectives [20] restricts the number of objective functions due to the single-objective nature of SDP that requires repeated scalarized single-objective optimizations for every Pareto optimal point, inducing a factorial growth of computation cost with the number of objectives [21,22].

The three curses of SDP limit its application in complex systems; therefore, over the years, a number of alternative methods have emerged, seeking to overcome one or more of these curses. Following the methodological classification proposed by [23,24], two main approaches can be distinguished:

(a) approximation in value space, which searches an approximation of the value function [25];

(b) approximation in policy space, which first defines the operating policy within a restricted class of parameterized functions and then explores the policy parameter space to optimize the system performance [26].

According to the recent review by [27], approximation in policy space and specifically the direct policy search (DPS) method is emerging as the most widely adopted method to advance water reservoir operations by overcoming both the curse of modeling and the curse of multiple objectives.

2.4.2 Evolutionary multi-objective direct policy search

Evolutionary multi-objective direct policy search (EMODPS) replaces the traditional SDP approach based on the computation of the value function, with a simulation-based optimization that directly operates in the policy space. EMODPS first parameterize the operating policy p_θ within a given family of functions and, then, explores the parameter space Θ seeking the best parameterization of the operating policy with respect to the expected long-term cost defined by the objectives of the problem, i.e.:

$$p_\theta^* = \; arg\, J_{p\theta} \qquad s.t. \quad \theta \in \Theta; \quad s_{t+1} = f_t(s_t, u_t, q_{t+1}) \qquad (10)$$

where the vector of objective functions J_{p_θ} is defined as in (3).

Finding p_θ^* corresponds to finding the best parameters θ^* for the class of policy p_θ, measured by the objectives J_{p_θ}. Notably, this formulation allows enlarging the decision vector to include additional variables beside the reservoir policy parameters, potentially including hedging rules parameters [28] and planning decisions [29,30].

A schematization of the EMODPS algorithm is reported in Figure 4. Because of the simulation-based nature of EMODPS, the variables domain does not need to be discretized, overcoming at once the curse of dimensionality and the biases introduced by the discretization of continuous variables [31]. Moreover, it is possible to couple DPS with exogenous information or models, thus avoiding the curse of modeling [6,32]. Finally, the use of MOEAs resolves to curse of multi-objective as EMODPS algorithms allow to produce an approximation of the Pareto front in a single run for up to 10 objectives [33].

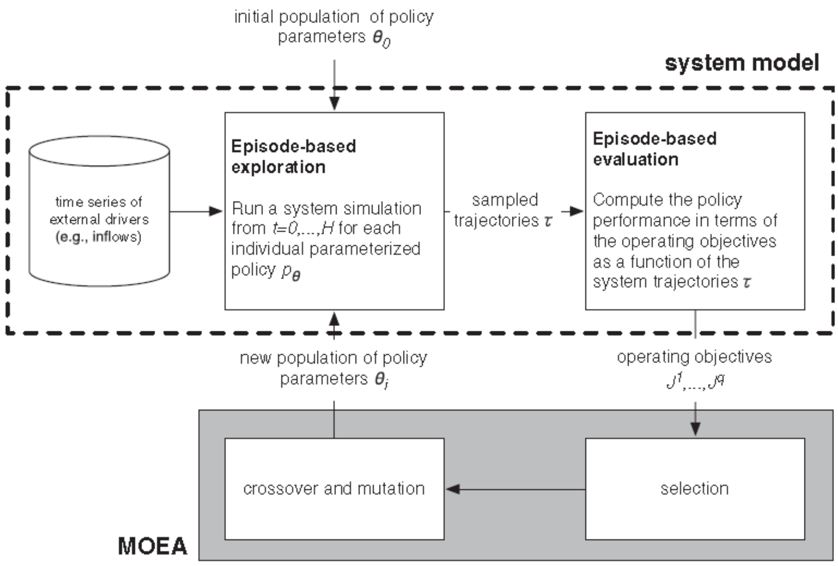

Figure 4 - Schematization of the Evolutionary Multi-Objective Direct Policy Search (EMODPS) approach; dashed lines represent the model of the system and the grey box represents the multi-objective evolutionary optimization algorithms (MOEA) [6]

2.4.3 Policy structure

EMODPS resolves a problem of parameters optimization for a given policy structure. It can therefore find, at most, the best possible solution for the chosen class of functions. When the system to be optimized is already operating, it is possible to infer the policy structure from the available data, although the water managers may not have operated at full attainable efficiency. If the system is under construction, neither data nor experience is available, and the policy structure must be guessed a priori on the basis of empirical considerations. The choice of a function with limited flexibility can thus restrict the search to a subspace of policies that, likely, does not contain the optimal one. It is hence advisable to select a very flexible class of functions, depending on a larger number of parameters, to ensure the possibility of approximating the unknown optimal solution of the problem to any desired degree of accuracy. Usually, the selected functions are universal approximating networks (for a review see [34] and references therein). Two widely used nonlinear universal approximators are artificial neural networks (ANNs) and radial basis functions (RBFs) [35]. It has been shown that any continuous function defined on a closed and bounded set can be approximated by three-layered ANNs [36,37] and three-layered RBFs [1,38].

Although ANNs are more popular in the field of water management then RBFs, a comparative analysis carried out in the Red River basin [39] shows the general superiority of RBF on ANN for the problem of parameterization of the operating policy. RBF policies computed for different time horizons consistently score better performances within a more reliable framework, i.e., without requiring any tuning or preconditioning of the policy design process. RBF thus represent an effective, case study-independent option for solving EMODPS problems and are therefore chosen as the universal approximation network for this study.

The RBF policy can be defined as follows:

$$u_t = \sum_{i=1}^{N} w_i \varphi_i(I_t) + a \qquad (11)$$

where N is number of RBFs $\varphi(\cdot)$ and w_i are the weight of the *i*-th RBF. A single RBF is defined as

$$\varphi_i(I_t) = exp\left[-\sum_{j=1}^{M} \frac{[(I_t)_j - c_{j,i}]^2}{b_{j,i}^2}\right] \qquad (12)$$

where M is the number of policy inputs I_t and c_i, b_i are the M-dimensional center and radius vectors of the i-th RBF, respectively. The centers of the RBF must lie within the bounded input space and the radii must strictly be positives i.e., using normalized variables, $c_i \in [-1, 1]$ and $b_i \in (0, 1]$. The parameter vector θ is therefore defined as $\theta = [a \; , c_{i,j}, b_{i,j}, w_i]$ with $i = 1, \ldots, N$, $j = 1, \ldots, M$, and it belongs to R^{n_θ}, where $n_\theta = N(2M + nu) + 1$.

2.4.4 Optimization algorithm – Borg MOEA

The two main options for the optimization step of the algorithm (the grey box in Figure 4) are gradient-based methods and global optimization algorithms, such as MOEAs. Simple parameterizations with few parameters are usually coupled with gradient-based methods, while global optimization algorithms are preferred when the number of parameters to optimize is high. MOEAs are iterative search algorithms that evolve a Pareto-approximate set of solutions by mimicking the randomized mating, selection, and mutation operations that occur in nature to drive the search for efficient solutions [40]. MOEAs have been shown to adapt well to multi-objective problems characterized by multi-modality, nonlinearity, stochasticity, and discreteness (see [41] and references therein). MOEAs thus represent a promising alternative to gradient-based optimization methods in solving complex multi-objective water reservoir problems. In addition, MOEAs were proven to better handle performance uncertainties than gradient-based methods [42].

To perform the optimization, in Task T4.3 we will use the self-adaptive Borg Multi-Objective Evolutionary Algorithm, which has been shown to be highly robust in solving multi-objective optimal control problems, where it met or exceeded the performance of other state-of-the-art MOEAs [43]. Borg MOEA differs from traditional evolutionary algorithms because the application of these operators is not bound to a fixed probability of occurrence. Their employment is adaptively adjusted during the optimization considering their ability to generate efficient solutions [44]. Along with the auto-adaptive search, Borg MOEA features other two strategies to contrast the main shortcomings of evolutionary algorithms: overfitting and poor exploration of the whole space when the search is trapped in a local minimum. The first strategy, the so-called ε-box dominance archive, divides the optimization space into hyper-boxes with side-length equal to ε. Pareto efficient solutions are searched into each box ensuring convergence. ε-box dominance also supports the second strategy: time continuation. Time continuation ensures a global search of the space by injecting mutated solutions in each ε-box. Stagnation in a local minimum is prevented with internal algorithmic operators that detect search stagnation, and randomly restart to escape local optima. Borg MOEA has been shown to outperform 9 benchmark evolutionary algorithms in terms of number of solutions returned, ability to handle many-objective problems, ease-of-use, and overall consistency across a suite of challenging multi-objective problems [45].

3. STRATEGIC MODEL FOR THE NILE RIVER BASIN

This section is dedicated to the description of the strategic model developed for the NRB, which integrates two main components:

- **Water Supply model** that supports the analysis of the operating policies of the main dams along the Nile River, along with the water abstraction for the irrigation areas in Sudan and the water supply downstream of the High Aswan Dam.
- **Water Demand model** that investigates alternative combinations of water demand interventions, namely reuse, groundwater, aquaponics/hydroponics and desalination, to reduce the water demand downstream of the High Aswan Dam.

3.1 WATER SUPPLY MODEL

The Water Supply model focuses on describing the branch of the Blue Nile from the Grand Ethiopian Renaissance Dam (GERD) to Khartoum and the Main Nile until it reaches the Mediterranean Sea (Fig. 5). In the system, three dams and four irrigation areas are modelled. The first dam is the GERD, situated in Ethiopia close to the border with Sudan, whose main purpose is the production of hydropower energy. The second dam is the Merowe dam (MER) in Sudan, built close to the border with Egypt to produce hydropower energy with an installed capacity of 1,250 MW.
The last downstream dam considered is the High Aswan Dam (HAD) in Egypt, which is used to supply water in the Nile Valley and Delta for irrigation, domestic and industrial uses, and it also produces hydropower energy with an installed capacity of 2,100 MW.

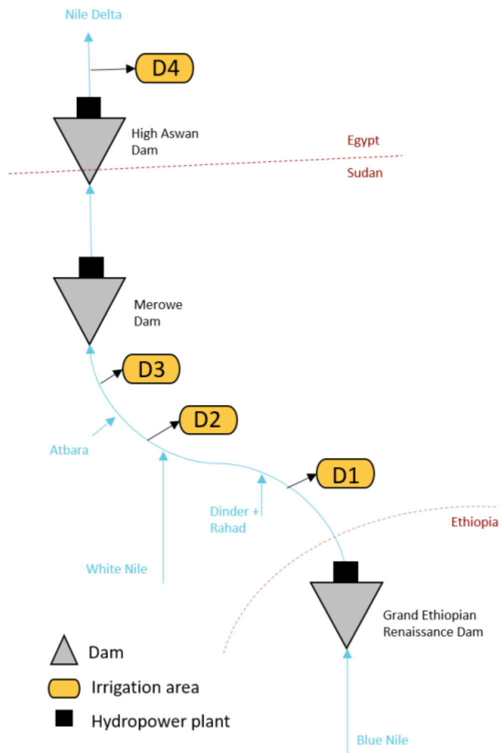

Figure 5 – Schematic representation of the model structure

The three reservoirs are modelled following a mass balance equation of the water storage with a monthly time step. The GERD's storage is formulated as follows:

$$S_{t+1}^{GERD} = S_t^{GERD} - R_{t+1}^1 - e_t^{GERD} * Sur_t^{GERD} + Q_{t+1}^1 \qquad (13)$$

where:

- S_t^{GERD} is the reservoir's storage at time t;
- e_t^{GERD} is the monthly net evaporation;
- Sur_t^{GERD} is the lake surface at time t;
- R_{t+1}^1 is the release from the GERD;
- Q_{t+1}^1 is the reservoir inflow.

The second reservoir, associated with the Merowe Dam, is modelled with the following equation:

$$S_{t+1}^{MER} = S_t^{MER} - R_{t+1}^2 - e_t^{MER} * Sur_t^{MER} + Q_{t+1}^{in} \qquad (14)$$

where:

- S_t^{MER} is the reservoir's storage at time t;
- e_t^{MER} is the monthly net evaporation;
- Sur_t^{MER} is the lake surface at time t;
- R_{t+1}^2 is the release from the Merowe Dam;

- $Q_{t+}^{in} = R_{t+1}^{1} + Q_{t+1}^{2} + Q_{t+1}^{3} + Q_{t+1}^{4} - I_{t+1}^{1} - I_{t+1}^{2} - I_{t+1}^{3}$ is the water flowing in the reservoir, it depends on the release from the GERD (R_{t+1}^{1}), on the water withdrawal of the irrigation areas in Sudan (I_{t+1}^{1}, I_{t+1}^{2}, I_{t+1}^{3}) and the inflows from Diner and Rahad (Q_{t+1}^{2}), White Nile (Q_{t+1}^{3}) and Atbara (Q_{t+1}^{4}).

Finally, the Lake Nasser water balance equation regulated by the HAD is formulated as follows:

$$S_{t+1}^{HAD} = S_{t}^{HAD} - R_{t+1}^{3} - R_{t+1}^{4} - e_{t}^{HAD} * Sur_{t}^{HAD} - Seep_{t+1} + R_{t+1}^{2} \qquad (15)$$

where:

- S_{t}^{HAD} is the reservoir's storage at time t;
- e_{t}^{HAD} is the monthly net evaporation;
- Sur_{t}^{HAD} is the lake surface at time t;
- R_{t+1}^{2} is the release from the Merowe Dam;
- $Seep_{t+1}$ represents the seepage and bank storage losses, which are modelled as a White Gaussian Noise [46];
- R_{t+1}^{3} is the release from the HAD;
- R_{t+1}^{4} is the release feeding the Toshka canal that is equal to the corresponding demand except when the water level of Lake Nasser is below 147 m a.s.l. and $R_{t+1}^{4} = 0$, or when the water level is above 178 m a.s.l. and then the spillway is activated.

According to the approach illustrated in Section 2.4, the operating policy determining the release decisions for the three dams are modelled as Gaussian Radial Basis Functions (RBFs):

$$R_{t+1}^{i} = RBF_{s}\left(Q_{t+1}^{1}, S_{t+1}^{GERD}, S_{t+1}^{Mer}, S_{t+1}^{HAD}, \tau_{t+1}\right) \qquad with\ i = 1,2,3 \qquad (16)$$

where:

- Q_{t+1}^{1} is the previous month inflow of the GERD reservoir;
- $S_{t}^{GERD}, S_{t}^{Mer}, S_{t}^{HAD}$ are respectively the storages of GERD, Merowe and HAD;
- τ_{t+1} is the month of the year

In the system, there are four main irrigation areas, three of which are in Sudan while one is in Egypt. The latter is subdivided into eleven different irrigation districts, and it is described in detail in Section 3.2.

The irrigation in Sudan is modelled using a diversion function (see eq. 2) that determines the water that is diverted to each irrigation district as follows:

$$I_{t+1}^{i} = f\left(Q_{t+1} - En_{t}, \omega_{t}^{i}, a_{i}, b_{i}\right) \qquad with\ i = 1,2,3 \qquad (17)$$

where:

- $Q_{t+1} - En_{t}$ is the water available for agriculture, namely the water flowing in the river (Q_{t+1}) decreased of the environmental flow (En_{t});
- ω_{t}^{i} is the demand of each district in Sudan;
- a_{i} , b_{i} are parameters defining the shape of the functions.

3.2 WATER DEMAND MODEL

The last stretch of the river, flowing from the HAD to the Mediterranean Sea, is characterized by the presence of eleven irrigation districts, whose water demand can be satisfied by the water released by the HAD or through the implementation of different water demand measures, namely water reuse, groundwater, hydroponics/aquaponics and desalination.

The irrigation districts are identified as areas of influence of eleven irrigation canals branching from eight barrages present on the river. The eleven considered canals are Asfoun, Kelabia, West Naga, East Naga, Ibrahimia, Tawfiki, Ismalia, Sharkawia, Menufia, Beheria and Nasseri (see Figure 6).

The current water demand of the eleven districts is 62.15 BCM/y [47]. The water demand distribution of each district (Tab. 1) is obtained through the scheme of the irrigation withdrawal distribution reported by [48].

Table 1 – Distribution coefficient of the irrigation demand downstream of Aswan

Number	Canal	Distribution coefficients α(%)
1	Asfoun	1.36
2	Kelabia	3.27
3	West Naga	7.63
4	East Naga	2.72
5	Ibrahimia	26.16
6	Tawfiki	10.63
7	Ismaila	10.63
8	Sharkawia	1.91
9	Menufia	13.08
10	Beheria	16.62
11	Nasseri	5.99

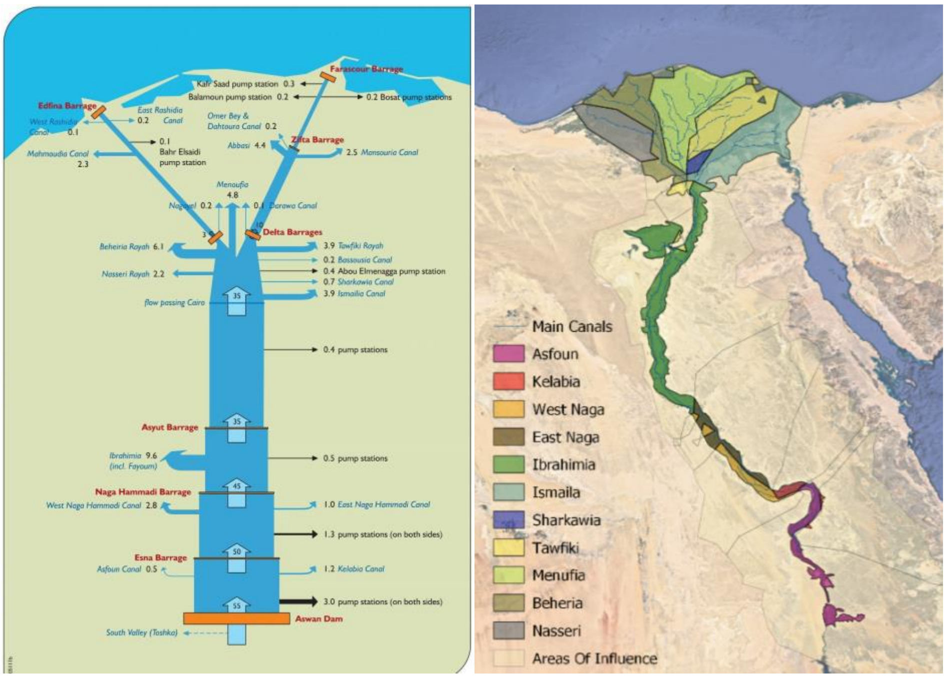

(a) (b)

Figure 6 – (a) Water distribution Nile system[48] (b) Irrigation districts used in the model.

The decision variables in this model are the planned water reductions allocation to reuse, groundwater, hydroponics/aquaponics and desalination. Each district is associated with one decision variable to define the water reuse, one for the groundwater extracted and one for the implementation of hydroponics/aquaponics. Besides, an 11x11 matrix represents the decisions associated with the desalination technology. The element in row *d* and column *i* of the matrix defines the volume of desalinated water produced in the *d-th* district that is delivered to the *i-th* district. If the *d-th* row has all 11 elements equal to zero, this means that the *d-th* district will not construct a desalination plant. If the *i-th* column has all 11 elements equal to zero, this means that the *i-th* district is not using any desalinated water. The model accounts for a total of 154 planning decisions, designed as follows:

$$u^p = \left| u_i^R \; u_i^{GW} \; u_i^A \; u_{i,d}^D \right| \quad with\ i = 1, \dots, 11\ and\ d = 1, \dots, 11 \tag{18}$$

where:

- u_i^R is the water reused in the *i-th* district;
- u_i^{GW} is the groundwater extracted in the *i-th* district;
- u_i^A is the percentage of agricultural production shifted from traditional agriculture to hydroponics/aquaponics in the *i-th* district;
- $u_{i,d}^D$ is the desalinated water produced in the *d-th* district with a desalination plant and used in the *i-th* district.

The total volume of water demand reduction achieved by the four selected measures is γ_{tot}. We can assume to implement a prioritization rule where the industrial and municipal water demand is met first by desalination, then by considering the water saving of hydroponics/aquaponics. Conversely, groundwater and reuse are primarily used for the irrigation demand, along with the surplus of hydroponics/aquaponics and desalination in case their corresponding water volumes are greater than the municipal water demand (i.e., for very large water demand reductions exceeding the total municipal water demand equal to 380 m^3/s).

To simulate this rule, we can define two variables γ^a and γ^b, the first consisting of the volumes of water demand reduced by desalination ($u^{D\_I\&M}$) and hydroponics/aquaponics ($u^{Aq\_I\&M}$) and the second representing the volumes of reuse water (u^R), groundwater (u^{GW}) and any surplus of hydroponics/aquaponics (u^{Aq_sur}) and desalination (u^{D_sur}).

$$\gamma^a = u^{D\_I\&M} + u^{Aq\_I\&M} \qquad (19)$$

$$\gamma^b = u^R + u^{GW} + u^{Aq\_sur} + u^{D\_sur} \quad (20)$$

Where:

- $u^{D\_I\&M} = \min(w^{4a}, u^D)$;
- $u^{D\_sur} = u^D - u^{D\_I\&M}$;
- $u^{Aq\_I\&M} = \min(w^{4a} - u^{D\_I\&M}, u^{Aq})$;
- $u^{Aq\_sur} = u^{Aq} - u^{Aq\_I\&M}$

3.2.1 Hydroponics & Aquaponics

In this work, aquaponics was modelled by assuming a conversion of part of the agricultural production of lettuce from traditional farming to hydroponics. Lettuce is chosen as the reference crop because of its wide use in already existing aquaponics systems in Egypt [49]. It represents the most feasible option for implementing a transition from traditional agriculture to soilless agriculture. This will allow to compare the theoretical costs here computed with the actual costs encountered on the study site.

It is assumed that the water saved due to such switch is proportional to the percentage of lettuce production converted to soilless agriculture:

$$Q_i^A = \beta * u_i^A * I^L \quad with\ i = 1, \dots, 11 \qquad (21)$$

where β is the percentage of water saving of hydroponics/aquaponics compared to traditional agriculture and I^L is the water consumption of lettuce in traditional cultivation. Note that our model does not consider the water consumption for fish production. The use of aquaponics allows a water saving of 85/99% compared to traditional agriculture, in this work it is chosen equal to 90% [49–51]. The water consumption of lettuce is estimated considering it proportional to the area occupied by this crop. The water consumption per feddan is 4,456 m^3/y [48], since the area cultivated with lettuce is 10,000 feddan [47], the total water consumption of lettuce is 0.045 BCM/y.

3.3 EVALUATION INDICATORS

Several stakeholders with conflicting interests (e.g., hydropower production vs. irrigation deficit vs. environmental flow deficit) may be affected by the reservoir and irrigation system operations. In the AWESOME project, these conflicting interests are captured by a set of evaluation indicators which are evaluated via simulation within Task T4.2 and have been first presented in D4.1 (Tab. 2).

Table 2 – Evaluation indicators formulated for the meso level Decision Analytic Framework (DAF).

SECTOR	EVALUATION INDICATOR	LOCATION	MODEL
ENERGY	Total hydropower production at the basin scale	River basin	water supply model
ENERGY	Hydropower production of GERD	Ethiopia	water supply model
ENERGY	Hydropower production of Merowe dam	Sudan	water supply model
ENERGY	Hydropower production of High Aswan Dam	Egypt	water supply model
WATER/FOOD	Total irrigation deficit in the three districts in Sudan	Sudan	water supply model
WATER/FOOD	Water supply deficit in Egypt	Egypt	water supply model
WATER	Domestic water supply deficit	Egypt	water supply + water demand model
WATER/FOOD	Irrigation water supply deficit	Egypt	water supply + water demand model
FOOD	Construction and operation cost of soilless agricultural systems	Egypt or single district	water demand model
FOOD	Annual production of vegetables from soilless agricultural systems	Egypt or single district	water demand model
FOOD	Annual production of fish from aquaponics systems	Egypt or single district	water demand model
WATER	Water consumption and saving of soilless agricultural systems	Egypt or single district	water demand model
ENERGY	Energy consumption of soilless agricultural systems	Egypt or single district	water demand model
FOOD	Distance of soilless agricultural systems from large urban centers	Egypt or single district	water demand model
WATER	Construction and operation cost of desalination plants	Egypt or single district	water demand model
WATER	Desalination water supply cost (proxy)	Egypt or single district	water demand model
WATER	Desalination water distribution cost (proxy)	Egypt or single district	water demand model
ENERGY	Annual energy consumption of desalination plants	Egypt or single district	water demand model
WATER/ECOSYSTEM	Annual reuse of drainage water	Egypt or single district	water demand model
WATER/ECOSYSTEM	Annual use of groundwater	Egypt or single district	water demand model
ECOSYSTEM	Groundwater use distance from the sea to avoid saline water intrusion	Egypt or single district	water demand model

SECTOR	EVALUATION INDICATOR	LOCATION	MODEL
SUSTAINABILITY	Sustainability Index	Egypt	water supply model
SUSTAINABLE DEVELOPMENT GOAL 6	Level of water stress	River basin	water supply model
SUSTAINABLE DEVELOPMENT GOAL 6	Transboundary cooperation	River basin	water supply model

The formulation of these indicators is as follows:

- Total hydropower production at the basin scale (energy):

$$J^{E,TOT} = \sum_{i=1}^{3} \frac{1}{H}\left[\sum_{t=0}^{H-1} P_{t+1}^{i}\right] \qquad (22)$$

where P_{t+1}^{i} is the monthly hydropower production of one of the three reservoirs, calculated as $P_{t+1} = \eta g \gamma \underline{h_t} q_{t+1}^{turb}$, where η [-] is the efficiency of the turbines, g=9.81 [m/s^2] is the gravitational acceleration, γ=1000 [kg/m^3] is the water density, $\underline{h_t}$ [m] is the net hydraulic head, and q_{t+1}^{turb} [m^3/s] is the turbinated flow. The hydropower productions of the three plants are aggregated under the assumption of coordinated management of the three reservoirs. As the hydroelectric sector does not consume water, it is assumed that the maximum benefit for energy production can be obtained when the three countries cooperate.

- Hydropower production of GERD (energy):

$$J^{E,GERD} = \frac{1}{H}\left[\sum_{t=0}^{H-1} P_{t+1}^{1}\right] \qquad (23)$$

where P_{t+1}^{1} is the annual hydropower production of GERD calculated as $P_{t+1} = \eta g \gamma \underline{h_t} q_{t+1}^{turb}$, where η = 0.9 is the efficiency of the turbines, g=9.81 [m/s^2] is the gravitational acceleration, γ=1000 [kg/m^3] is the water density, $\underline{h_t}$ [m] is the net hydraulic head, and q_{t+1}^{turb} [m^3/s] is the turbinated flow.

- Hydropower production of Merowe Dam (energy):

$$J^{E,MER} = \frac{1}{H}\left[\sum_{t=0}^{H-1} P_{t+1}^{2}\right] \qquad (24)$$

where P_{t+1}^{2} is the annual hydropower production of Merowe Dam calculated as $P_{t+1} = \eta g \gamma \underline{h_t} q_{t+1}^{turb}$, where η = 0.9 is the efficiency of the turbines, g=9.81 [m/s^2] is the gravitational acceleration, γ=1000 [kg/m^3] is the water density, $\underline{h_t}$ [m] is the net hydraulic head, and q_{t+1}^{turb} [m^3/s] is the turbinated flow.

- Hydropower production of High Aswan Dam (energy):

$$J^{E,HAD} = \frac{1}{H}\left[\sum_{t=0}^{H-1} P_{t+1}^{3}\right] \qquad (25)$$

where P_{t+1}^{3} is the annual hydropower production of HAD calculated as $P_{t+1} = \eta g \gamma \underline{h_t} q_{t+1}^{turb}$, where η = 0.9 is the efficiency of the turbines, g=9.81 [m/s^2] is the gravitational acceleration, γ=1000 [kg/m^3] is the water density, $\underline{h_t}$ [m] is the net hydraulic head, and q_{t+1}^{turb} [m^3/s] is the turbinated flow.

- Total irrigation deficit in the three districts in Sudan (water/food):

$$J^{Irr,Sudan} = \sum_{i=1}^{3} \quad \frac{1}{Nyears} \sum_{t=0}^{H-1} \quad max\,(w_t^i - I_{t+1}^i, 0) \qquad (26)$$

where w_t^i is the irrigation demand of the *i-th* area located in Sudan and I_{t+1}^i is the water supplied to the *i-th* irrigation area.

- Water supply deficit in Egypt (water/food):

$$J^{Deficit,Egypt} = \frac{1}{Nyears} \sum_{t=0}^{H-1} \quad max\,(w_t^4 - \gamma_{tot} - R_{t+1}^3, 0) \quad (27)$$

where w_t^4 is the water demand downstream of HAD, γ_{tot} is the water demand reduction of the Egyptian agricultural sector obtained through the implementation of water reuse, groundwater, hydroponics/aquaponics and desalination, and R_{t+1}^3 is the water released by HAD.

- Municipal and industrial water supply deficit (water):

$$J^{M\&I,Egypt} = \frac{1}{Nyears} \sum_{t=0}^{H-1} \quad max\,(w_t^{4a} \; - \gamma^a(u^D, u^A) - \; R_{t+1}^3, 0) \quad (28)$$

where w_t^{4a} is the municipal and industrial water demand downstream of HAD, $\gamma^a(u^D, u^A)$ is the water demand reduction allocated to the municipal and industrial demand and R_{t+1}^3 is the water released by HAD.

- Irrigation water supply deficit in Egypt (water/food):

$$J^{Irr,Egypt} = \frac{1}{Nyears} \sum_{t=0}^{H-1} \quad max\,(w_t^{4b} - \; \gamma^b(u^R, u^{GW}, u^A, u^D) - max(R_{t+1}^3 - w_t^{4a} - \gamma^a(u^D, u^A), 0), 0) \qquad (29)$$

where w_t^{4b} is the irrigation demand downstream of HAD (with w_t^{4a}+w_t^{4b}= w_t^4), $\gamma^b(u^R, u^{GW}, u^A, u^D)$ is the water demand reduction of the Egyptian agricultural sector, and R_{t+1}^3 is the water released by HAD.

- Construction and operation cost of soilless agricultural systems (food):

$$J^{Aq1} = \sum_{i=1}^{11} \quad [CAPEX(S_i^*) + OPEX(S_i^*) * Nyears] \quad (30)$$

$$CAPEX(S_i^*) = \begin{cases} 0 & if\; u_i^A{=}0 \\ CAPEX & if\; u_i^A{\neq}0 \end{cases} \qquad (31)$$

$$OPEX(S_i^*) = \begin{cases} 0 & if\; u_i^A{=}0 \\ OPEX & if\; u_i^A{\neq}0 \end{cases} \qquad (32)$$

where $S_i^*(P_i^*)$ is the size of the hydroponics/aquaponics expected to produce P_i^*, P_i^* is the production target for the hydroponics/aquaponics system in the *i-th* district calculated as $P_i^* = u_i^A * P^L$, where P^L is the average annual production of lettuce from traditional agriculture equals 87,000 tn[47].

- Annual production of vegetables from soilless agricultural systems (food):

$$J^{Aq2} = \sum_{i=1}^{11} \quad u_i^A * P^L \qquad (33)$$

where P^L is the average annual production of lettuce from traditional agriculture equals 87,000 tn [47].

- Annual production of fish from hydroponics/aquaponics systems (food):

$$J^{Aq3} = \sum_{i=1}^{11} S_i^*(P_i^*) * P^F \qquad (34)$$

where $S_i^*(P_i^*)$ is the size of the hydroponics/aquaponics expected to produce P_i^* and P^F is the fish revenue of an aquaponics system of one acre set at 11 tn as estimated by [49].

- Water consumption and saving of soilless agricultural systems (water):

$$J^{Aq4} = \sum_{i=1}^{11} (1-\beta) * u_i^A * I^L \qquad (35)$$
$$J^{Aq5} = \sum_{i=1}^{11} \beta * u_i^A * I^L \qquad (36)$$

where β is the percentage of water saving of hydroponics/aquaponics compared to traditional agriculture and I^L is the water consumption of lettuce in traditional cultivation. The use of hydroponics/aquaponics allows a water saving of 85/99% compared to traditional agriculture, in this work it is chosen equal to 90% [49–51].

- Energy consumption of soilless agricultural systems (energy):

$$J^{Aq6} = \sum_{i=1}^{11} S_i^*(P_i^*) * E^{Aq} \qquad (37)$$

where $S_i^*(P_i^*)$ is the size of the hydroponics/aquaponics expected to produce P_i^* and $E^{Aq}$is the annual energy consumption of a hydroponics/aquaponics system of one cubic metre equal to 47.36 kWh (information derived from the AWESOME pilot scale).

- Average distance of lettuce production from large urban centers (food):

$$J^{Aq7} = \sum_{i=1}^{11} \lambda_i \times d_i^{Aq} \quad (38)$$

where d_i^{Aq} is the distance, in km of roads, of the *i-th* district centroid from the most densely populated area represented by Cairo and the lands around it, which is weighted according to the lettuce production in the *i*-th district (P_i) with respect to the total production (P_{tot}) by using $\lambda_i = P_i/P_{tot}$.

- Construction and operation cost of desalination plants (water):

$$J^{D1} = \sum_{d=1}^{11} \left[\sum_{i=1}^{11} \left(u_{d,i}^D\right) * UPC\left(\sum_{i=1}^{11} u_{d,i}^D\right) * Nyears\right] \qquad (39)$$

where $UPC\left(\sum_{i=1}^{11} u_{d,i}^D\right)$ is the function expressing the unit process costs according to the desalination capacity. The function aggregates construction and operational costs amortizing them over the average life expectancy of a plant [52]. Note that our model does not detail the brine management and its implications in terms of environmental impacts and economic costs.

- Desalination water supply proxy cost (water):

$$J^{D2} = \sum_{i=1}^{11} d_i^{Sea} \quad if \sum_{d=1}^{11} u_{i,d}^D \neq 0 \qquad (40)$$

where d_i^{Sea} is the distance of a district containing a desalination plant from the sea.

- Desalination water distribution proxy cost (water):

$$J^{D3} = \sum_{i=1}^{11} \quad d_{i,d} \quad if\ u_{i,d}^{D} \neq 0 \qquad (41)$$

- Annual energy consumption of desalination plants (energy):

$$J^{D4} = \sum_{i=1}^{11} \quad [\sum_{d=1}^{11} \quad (u_{i,d}^{D}) * E^{D}] \qquad (42)$$

where E^D is the energy consumed by a desalination plant, assuming that the desalination plant uses the reverse osmosis (RO) technology with an energy recovery system E^D = 3 kWh/m^3 according to [53–55].

- Annual reuse of drainage water (water/ecosystem):

$$J^{R} = \sum_{i=1}^{11} \quad u_{i}^{R} \qquad (43)$$

where u_i^R is the drainage water reused in the *i-th* district.

- Annual use of groundwater (water/ecosystem):

$$J^{GW1} = \sum_{i=1}^{11} \quad u_{i}^{GW} \qquad (44)$$

where u_i^{GW} is the groundwater extracted in the *i-th* district.

- Groundwater use distance from the sea to avoid saline water intrusion (ecosystem):

$$J^{GW2} = \sum_{i=1}^{11} \quad \frac{u_{i}^{GW}}{d_{i}^{Sea}} \qquad (45)$$

where u_i^{GW} is the groundwater extracted in the *i-th* district and d_i^{Sea} is the distance of the *i-th* district from the coast.

- Sustainability Index (sustainability): it is an integration of performance criteria that capture the essential and desired sustainable characteristics of alternative water supply policies from the perspective of water users [56].It is formulated as follows:

$$J^{SI1} = [Rel \times Res \times (1 - Vul)]^{1/3} \qquad (46)$$

where Rel is the water demand reliability computed as the probability that the available water supply meets the water demand during the period of simulation.

$$Rel \quad = \frac{No.of\ times\ D_t^E = 0}{n} \qquad (47)$$

where D_t^E is the Egyptian water deficit and n is the number of months considered in the simulation.
Res is the resilience, namely the system's capacity to adapt to changing conditions, calculated as:

$$Res \quad = \frac{No.of\ times\ D_t^E = 0\ follows\ D_t^E > 0}{No.of\ times\ D_t^E > 0\ occurred} \qquad (48)$$

and Vul is the vulnerability, the likely value of deficits, if they occur, computed as:

$$Vul \quad = \frac{\sum_t \quad D_t^E{}_t\ /\ No.of\ times\ D_t^E > 0\ occurred}{water\ demand} \qquad (49)$$

- Level of water stress (Sustainability Development Goal (SDG) 6.4.2): The Indicator 6.4.2 tracks how much freshwater that is being withdrawn by all economic activities, compared to the total renewable freshwater resources available, after taking into account environmental flows. This indicator is also known as water withdrawal intensity and will measure progress towards SDG Target 6.4. It can be computed as:

$$J^{WS} = \frac{\frac{1}{Nyears}\sum_t \sum_i I_t^i + \frac{1}{Nyears}\sum_t R_t^3}{(total\ water\ availability + \gamma_{tot})} \quad (50)$$

where I_t^i is the water diverted to the i-th irrigation area of Sudan, R_t^3 is the water released by HAD, the total water available is considered as the annual total inflow of the Nile and γ_{tot} is the water demand reduction.
Data per country and status (2018) can be found here[57].

- Transboundary cooperation (SDG 6.5.2): Transboundary water cooperation plays a crucial role in supporting wider regional integration, peace and sustainable development, as well as in tackling regional security challenges and in supporting climate change adaptation. The Indicator 6.5.2 tracks the percentage of transboundary basin area within a country that has an arrangement for water cooperation is a bilateral or multilateral treaty, convention, agreement or other formal arrangement between riparian countries that provides a framework for cooperation. For the arrangement to be considered operational, the following criteria need to be fulfilled:
    - Existence of a joint body.
    - Regular, formal communication between riparian countries (at least once a year).
    - Joint or coordinated management plans or objectives.
    - Regular exchange of data and information (at least once a year).
    - Data are commonly compiled by relevant national line ministries and institutions (e.g. for Water, Environment, Natural Resources, Hydrology, Geology).

  The world status data indicating the proportion of transboundary basin area with an operational arrangement for water cooperation (per country) can be found here [58].

4. ANALYSIS/EVALUATION OF SELECTED PLANNING PORTFOLIOS

In this section, the simulation results of some candidate portfolios for the water supply and water demand models are presented. First, the water supply simulation is discussed analyzing three alternatives: one that maximizes the indicator for hydropower production at the basin scale (J^{E}), one that minimizes the total deficit of Egypt ($J^{Deficit,Egypt}$) and the last that minimizes the Sudanese one ($J^{Irr,Sudan}$). Similarly, the water demand model is then simulated for three different alternatives corresponding to different combinations of water demand interventions.

4.1 WATER SUPPLY PORTFOLIOS

The simulation results of the water supply model are displayed in Figure 7 in a parallel axes plot. This consists of an 8-dimensional space, where the axes represent the evaluation indicators simulated by the water supply model (Table 2). This parallel-coordinate plot representation shows each portfolio as a line crossing the eight axes at the values of their corresponding performance. In the plot, the indicator values are reported between their minimum and maximum values and the axes are oriented so that the direction of preference is always upward. Consequently, the ideal solution would be a horizontal line running along the tops of all of the axes. The conflicts are designated as diagonal lines between two adjacent axes. Looking at the extremes of the figure the production of hydropower in GERD exceeds the production of the other two dams, while the hydropower productions of Merowe and HAD have similar values. However, the installed capacity of the GERD is indeed greater than all the other hydropower systems in the NRB.

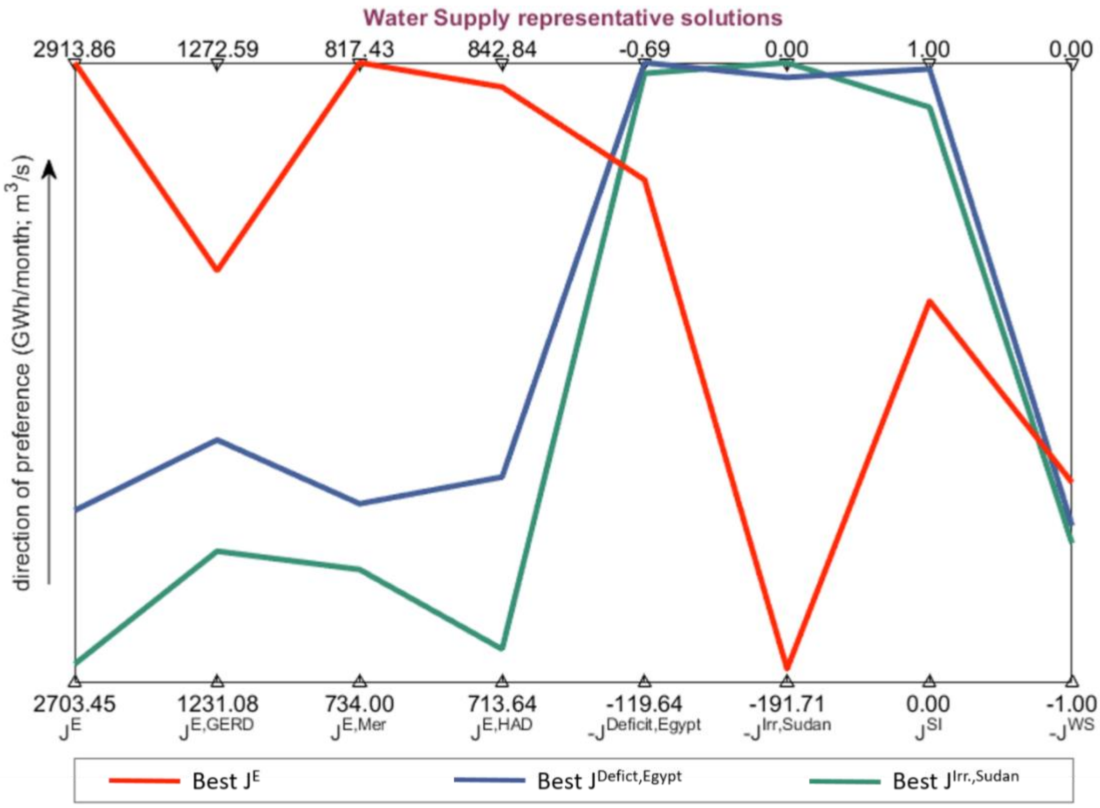

Figure 7– Representative solution for the water supply model. The three solutions are represented in the objective space and each solution maximize one of the indices J^{E}, $J^{Deficit,Egypt}$ and $J^{Irr,Sudan}$

The three lines (red, blue, green) represented in Figure 7 correspond to three candidate portfolios in which the selected indicators J^{E}, $J^{Deficit,Egypt}$ and $J^{Irr,Sudan}$ are independently maximized. The first portfolio (red line) maximizes the hydropower production at the basin scale. For this solution the hydropower production in all the three reservoirs is high, showing that there is not a strong conflict between the hydropower sector of the three countries. This sector does not consume water, which allows high hydroelectric revenues to be achieved in all three countries. To maximize hydropower production, this portfolio, however, produces a large deficit in the Sudanese agricultural sector as shown by the value of the $J^{Irr,Sudan}$ indicator. This contrast is caused by the consumptive use nature of the agricultural sector: when water is used for irrigation in Sudan, it is no longer available for hydropower production in Merowe and HAD. Egypt's water deficit does not drop as low as the Sudanese one, as all of the Egyptian water demand is located downstream of the three dams and the corresponding water consumption does not influence hydroelectric production. Moreover, this portfolio is associated to a reduction of 5.5% of the Egyptian water demand.

The second considered portfolio (blue line) is the best alternative for the water deficit of Egypt. Interestingly, the irrigation sectors of Egypt and Sudan do not appear conflicting despite the Sudanese diversions are upstream of the Egyptian agricultural area. This result could be explained by the contributions of the water demand measures, as this solution is characterized by a value of γ_{tot} of 125 m^3/s (5.8% of the Egyptian water demand). These measures make high water consumption possible in the irrigation sectors of both countries. Compared to the previous one, this portfolio shows a strong degradation in the performance of the indicators for hydropower production. This is mainly attributable to the low irrigation deficit in Sudan, which, as already mentioned, is located upstream of two of the three dams in the system and subtracts water from power production.

The third portfolio (green line) is the best alternative for the water deficit of Sudan. This portfolio has a similar pattern to the previous one. In this case, the low water deficits for both countries is attained by requiring a water demand reduction in Egypt equal to 1% of the total demand of the country. Again, it is clear how low deficits for irrigation lead to poor performance of the energy sector.

In addition to hydropower production and water deficits, the last two axes report the values of the sustainability and water stress indicators expressed as fractions from 0 to 1. The first indicator is strongly correlated to the deficit level of Egypt, with the solution with lowest $J^{Deficit,Egypt}$ performing the best also in J^{SI}. The water stress indicates the percentage of water withdrawal compared to the water availability for Egypt and Sudan, with the values reported with negative values so that the best performances are at the top of the graph. All three portfolios show high values of water stress between 68 and 77%, numbers that do not surprise for countries affected by arid climate conditions and high water demands. The indicator is lower compared to the values reported in[57]. This difference is due to the fact that industrial and municipal water demand was not taken into account for Sudan due to a lack of data. Finally, all three solutions assume full cooperation between states, implying that the entire considerate area of the basin is under an operational arrangement for water cooperation.

The three selected portfolios can be further analyzed looking at the dynamics of the three reservoirs. In Figure 8, the monthly and annual trajectories of the water levels of HAD, Merowe dam and GERD are reported. The water level of HAD varies with the considered solutions more evidently than the other reservoirs, especially during dry years. For example, the solution with best J^E mainly increases the water level of HAD instead of GERD, although HAD reservoir has much less installed capacity than GERD. The solution with best $J^{Irr,Sudan}$ decreases significantly the HAD water level, especially in wet seasons and dry years, as water is consumed upstream of the dam. In contrast, the solution with best $J^{Deficit,Egypt}$ tends to keep high reservoir water levels, which ensures enough water for the irrigation sector and hydropower production during dry seasons.

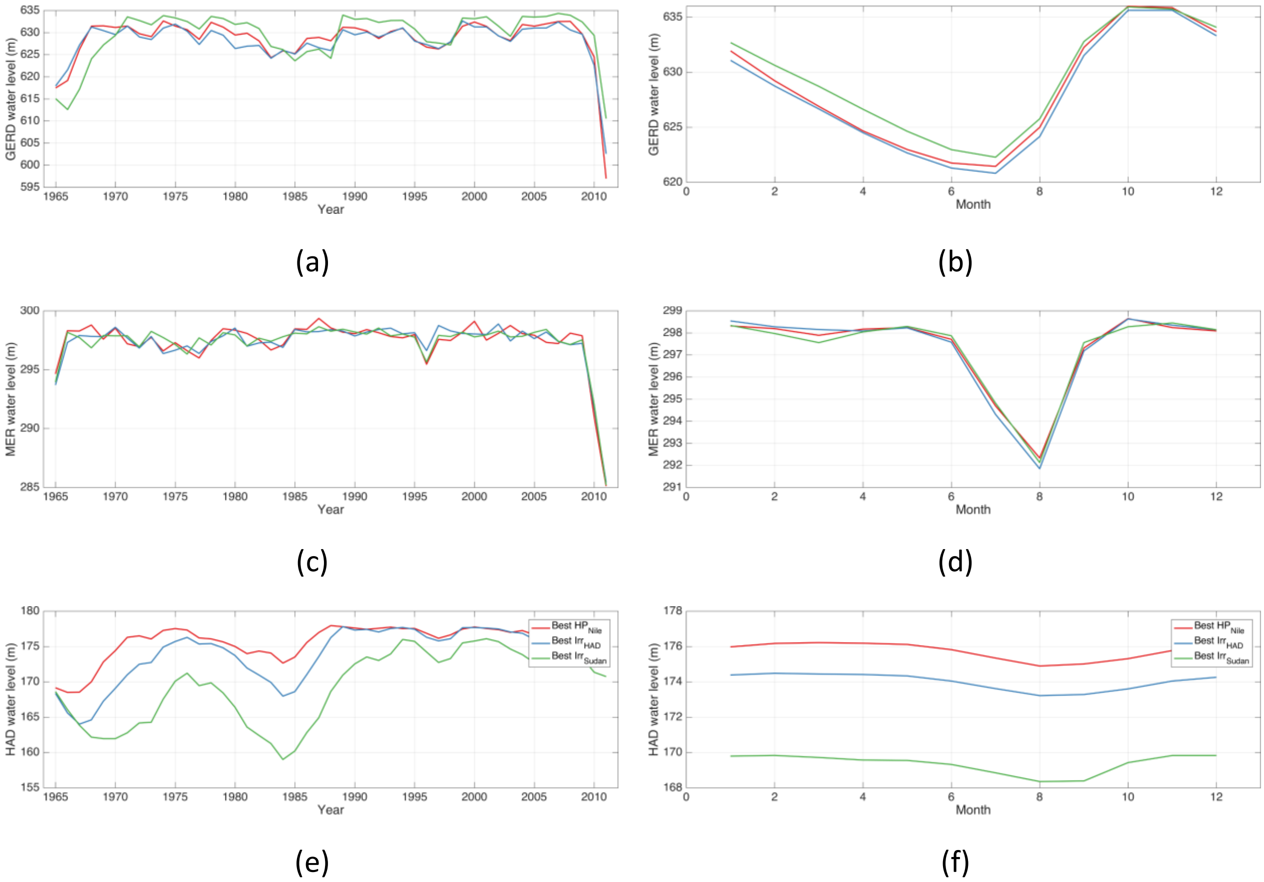

Figure 8 - Monthly (left) and annual (right) Grand Ethiopian Renaissance Dam (GERD), Merowe Dam (MER), and High Aswan Dam (HAD) water level trajectories of representative policies in Nile operation.

4.2 WATER DEMAND PORTFOLIOS

In this section, we analyze the impacts of water demand reduction portfolios on the system downstream of HAD. The selected portfolios defines a combination of drainage reuse, groundwater extraction, aquaponics and desalination plants.

Starting from an arbitrary water demand reduction (γ_{tot}= 22 m^3/s) chosen as target for the second problem, three solutions are simulated with the water demand model. The results are firstly shown as volumes of water allocated to each measure in Figure 9. The values at the top of the axes show the maximum exploitation of the four measures. Reuse, groundwater and desalination reach similar maximum values, while aquaponics has a more limited range due to its restricted implementation in the model. Assuming that all lettuce cultivation is converted from conventional farming to aquaponics, it is achieved a maximum water saving of 90% of 0.045 BCM/y, (i.e. the amount of water currently consumed by the lettuce crop). The first portfolio, marked with light blue, is selected as a solution with a maximum exploitation of aquaponics. Since the contribution of aquaponics is limited, this solution is still characterized by high volumes of the other measures, in particular reuse and groundwater. The second portfolio (yellow line) is selected as representative of a large implementation of desalination. As this technology is not physically limited, in this portfolio the water volumes saved by the other measures are small. Lastly, the third considered portfolio (red line) represents a low-cost alternative that relies on water reuse and groundwater only. Both desalination and aquaponics indeed require high costs for infrastructure development, unlike reuse and groundwater, which are already widely used in the area. However, this portfolio has the strong disadvantage of being less environmentally sustainable due to the high consumption of drainage water and groundwater.

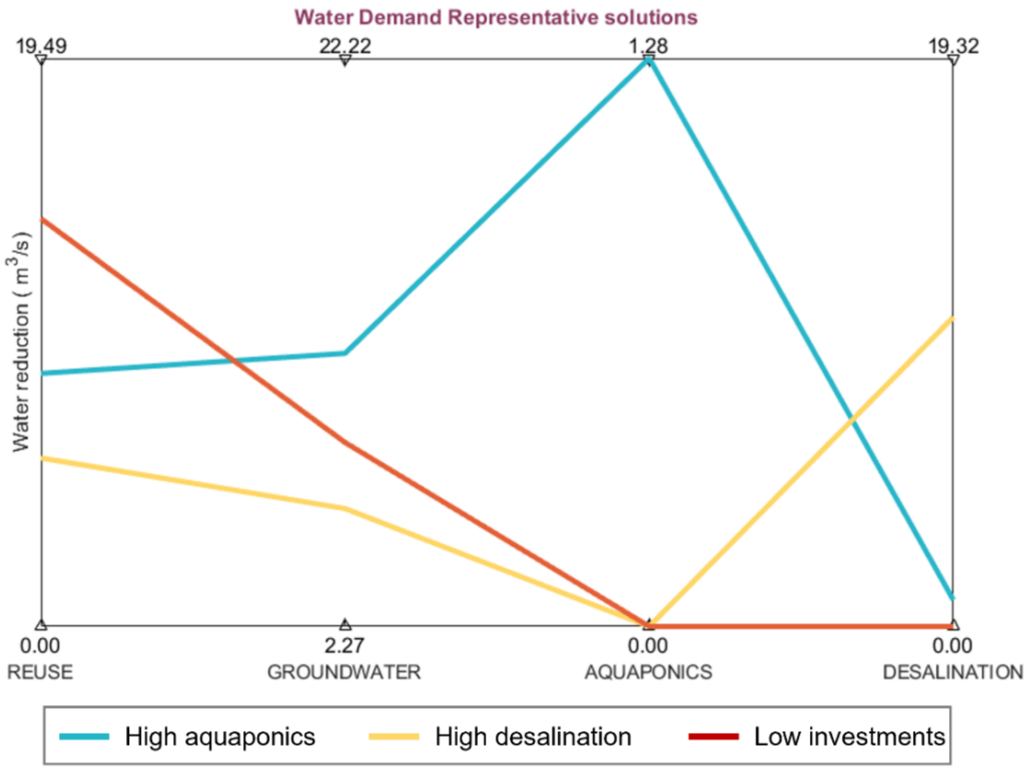

Figure 9 - Representative solution for the water demand model. The three solutions are represented as volumes allocated to the selected measures (reuse, groundwater, aquaponics and desalination).

The values of the evaluation indicators for the three portfolios were computed via simulation of the water demand model and are illustrated in the parallel axes in Figure 10. As in Figure 7, this parallel axes plot reports on the horizontal axes the maximum and minimum values of the indicators. Each portfolio is represented as a line crossing the fourteen axes at the values of their corresponding performance, with the axes that are oriented so that the direction of preference is always upwards.

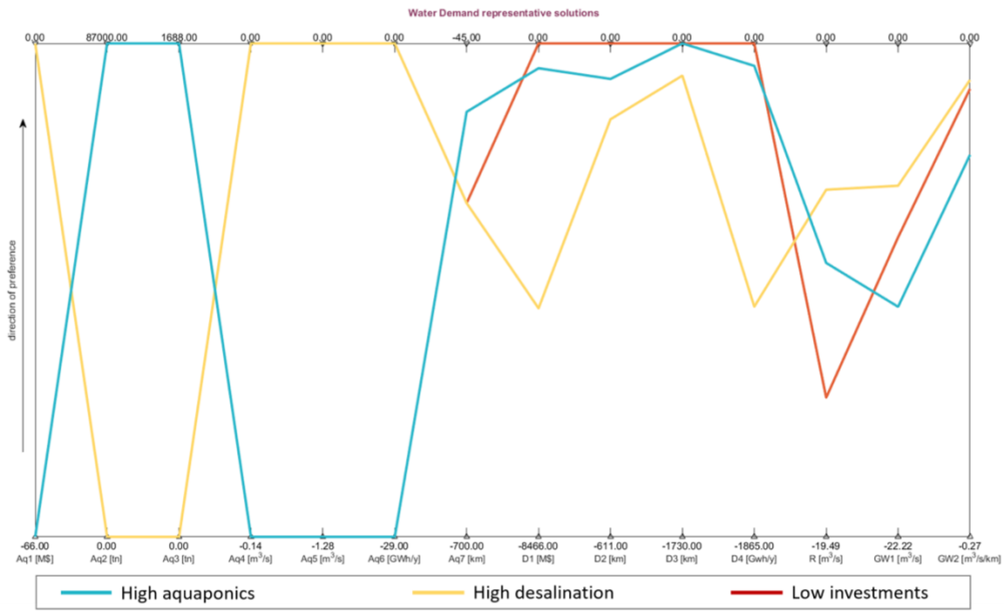

Figure 10- Performance of three candidate portfolios simulated by the water demand model.

The portfolio for high aquaponics exploits the maximum implementation of this measure, as is shown by the attainment of maximum values of aquaponics costs, lettuce and fish production, energy consumption and water savings. This solution implies a major effort to implement aquaponics systems since all lettuce production in the country would switch from traditional farming to aquaponics. Moreover, the implemented systems appear to improve the location of lettuce cultures compared to the current situation, allocating them closer to the most densely populated area, as shown by the value of the indicator J^{Aq7} close to the upper bound of the axes. This solution also involves the construction of a desalination unit of medium capacity (around 80,000 m^3/d). The investment required by this plant amounts to 426 M$ for an operating horizon of 30 years, which is higher than the investment required by aquaponics, equivalent to 66 M$ for the same period. The energy consumption of the desalination unit (85 GWh/y) is also higher than the one expected from aquaponics (29 GWh/y). Notably, in this portfolio the implementation of aquaponics is contributing a higher water saving than desalination while also being preferable in terms of both investment costs and energy consumption. This is due to the fact that desalination plants become competitive for larger capacities, as the operational costs of these plants decrease as desalinated water produced increases [52]. The portfolio associated to high desalination involves the construction of two desalination plants of 800,000 m^3/d and 120,000 m^3/d. These require a total investment of 4,545 M$ over the span of 30 years and an annual energy consumption of 995 GWh. The low investment portfolio achieves all the minimum values for the implementation costs of

aquaponics and desalination, as it does not exploit these two measures, but presents high values for the indicators related to reuse and groundwater.
Looking at the values of $J^{M\&I,Egypt}$ and $J^{Irr,Egypt}$, all three solutions have municipal and industrial deficits equal to zero and the deficits for irrigation equal to 1.95 m^3/s. This happens because all portfolios are derived from the same water supply simulation, so they are all characterized by the same deficit. Furthermore, the municipal deficit is always zero for low deficit solutions since municipal demand is much lower than the irrigation one. Simulating the model according to future scenarios with increasing demand and decreasing water availability, alternatives with non-zero industrial and municipal deficits could occur. In the three selected solutions, all the desalinated water and water saved due to aquaponics are used to reduce municipal and industrial demand. The alternatives with high aquaponics and low investments allocate most of the water reductions, characterized by high values of reuse and groundwater, to the irrigation sector. In the solution with high desalination almost half of the water reduction is sustained by desalination, which serves the municipal and industrial water demand, and the other half of the water reduction is met by reuse and groundwater that serves the irrigation demand.

To better understand what happens in each district, the three portfolios are further unraveled. Figure 11 shows the spatial distribution of the four water demand measures in the eleven irrigation districts. Some similarities between the three alternatives can be observed. The use of groundwater is prevalent in the first five districts, all of which are outside the Delta thus producing low environmental risks related to seawater intrusion. An exception is the first portfolio which is using groundwater in two coastal districts to produce the highest use of groundwater for completing the limited saving from the aquaponics technology. In the high aquaponics portfolio, two aquaponics systems are implemented, one being located in district 8 (Sharkawia) the closest to Cairo. The alternative also involves a medium-sized desalination unit in the ninth district (Menufia). The portfolio with high desalination shows a predominant use of desalinated water in the Delta, with the construction of two large desalination plants in districts 9 (Menufia) and 11 (Nasseri). The plant in the ninth district supplies water to the two adjacent districts 6 (Tawfiki) and 10 (Beheria). The last portfolio requiring low investments uses only groundwater and reuse, the first one used in the Nile Valley while the second in the Delta. Yet, this solution generates high environmental risks for the use of water of low quality and the potential intrusion of saline water.

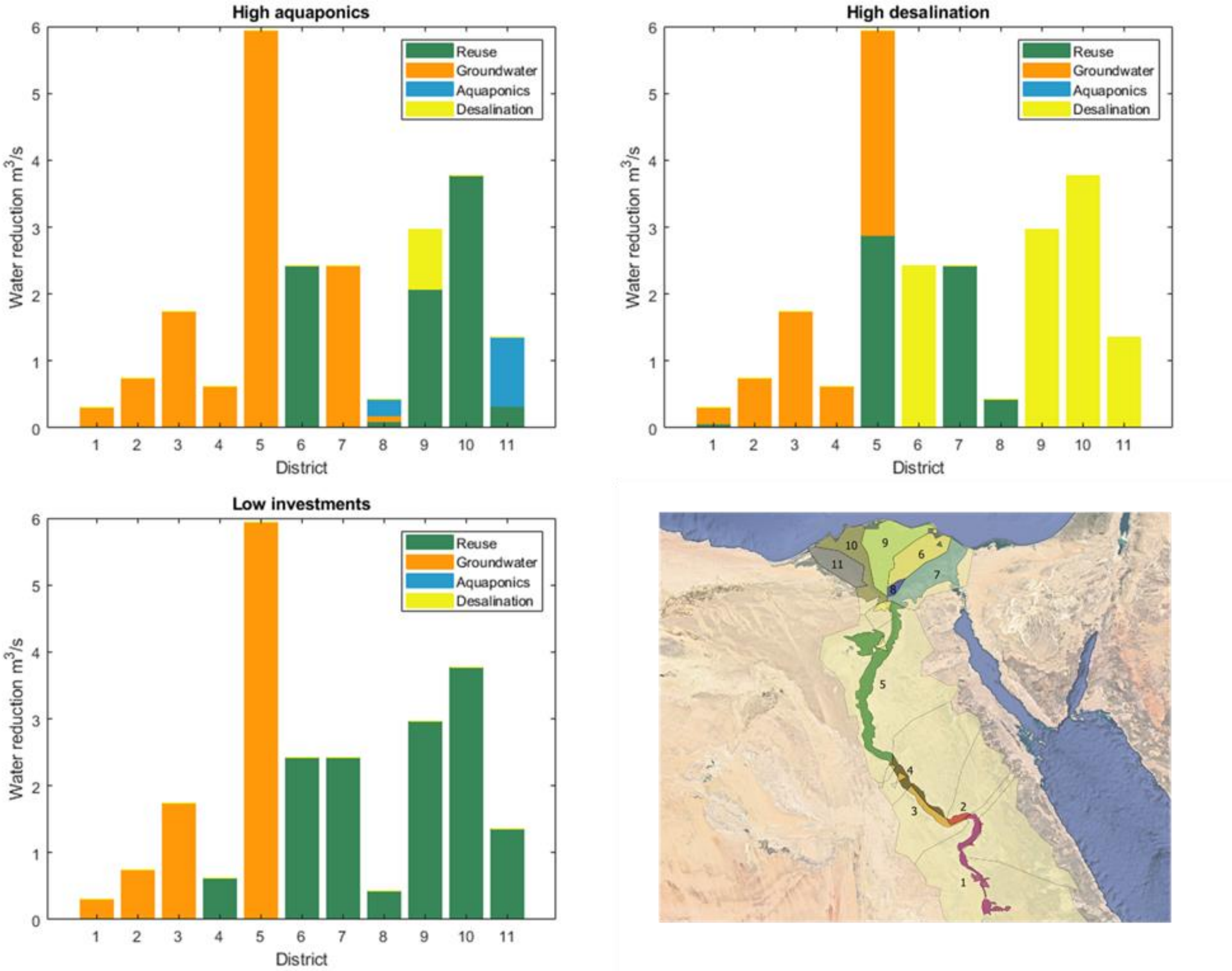

Figure 11- Spatial distribution of water demand reduction measures for the three selected solutions. The districts are reported on the horizontal axis and in the right bottom figure with numbers from 1 to 11: (1) Asfoun, (2) Kelabia, (3) West Naga, (4) East Naga, (5) Ibrahimia, (6) Tawfiki, (7) Ismaila (8) Sharkawia, (9) Menufia, (10) Beheria, (11) Nasseri.

5. FINAL REMARKS AND NEXT STEPS

This deliverable illustrates the strategic meso level model of the NRB, which represents a key component of the DAF for discovering multi-sectoral synergies and trade-offs by exploring the multi-dimensional space of the evaluation indicators formulated in Deliverable D4.1.

Key findings about the water supply model indicate a clear trade-off between hydropower production and irrigation abstraction in Sudan. In addition, the considered portfolios do not show substantial conflicts between irrigation in Egypt and Sudan. As for the water demand, the portfolios analyzed in this report show that the introduction of advanced water demand technologies such as aquaponics and desalination can reduce water demands, but they require high initial investments.

Similar water demand reductions can be obtained at lower costs by increasing water reuse and groundwater pumping, but this strategy has high environmental risks.

In the next developments, the candidate portfolios described in this report will be further explored under current and future scenarios of water availability, demands, and regional policies as suggested by the other WPs at the different levels/scales. Specifically, WP2/3 will provide inputs to the DAF related to future inflows according to different climate change projections, along with the associated projections of the irrigation demands. In addition, the energy system model will provide information about the national/river basin hydropower production strategies, while the Computable General Equilibrium model will support the economic assessment of the different water demand technologies. Lastly, WP5 will provide more detailed information to characterize the hydroponics/aquaponics technologies based on the AWESOME demo site.

REFERENCES

1. Maier, H. R. *et al.* Evolutionary algorithms and other metaheuristics in water resources: Current status, research challenges and future directions. *Environmental Modelling & Software* **62**, 271–299 (2014).
2. Piccardi, C. & Soncini-Sessa, R. Stochastic dynamic programming for reservoir optimal control: Dense discretization and inflow correlation assumption made possible by parallel computing. *Water Resour Res* **27**, 729–741 (1991).
3. Celeste, A. B. & Billib, M. Evaluation of stochastic reservoir operation optimization models. *Adv Water Resour* **32**, 1429–1443 (2009).
4. Yeh, W. W. Reservoir management and operations models: A state-of-the-art review. *Water Resour Res* **21**, 1797–1818 (1985).
5. Bellman Rand Corporation., R. *Dynamic programming*. (Princeton University Press, 1957).
6. Giuliani, M., Castelletti, A., Pianosi, F., Mason, E. & Reed, P. M. Curses, Tradeoffs, and Scalable Management: Advancing Evolutionary Multiobjective Direct Policy Search to Improve Water Reservoir Operations. *J Water Resour Plan Manag* **142**, 04015050 (2016).
7. Hall, W. A. & Buras, N. The dynamic programming approach to water-resources development. *J Geophys Res* **66**, 517–520 (1961).
8. MAASS, A. *et al.* Design of Water Resource System. *Soil Sci* **94**, (1962).
9. Esogbue National Science Foundation (U.S.) Special Workshop on Dynamic Programming and Water Resources, A. O. Dynamic programming for optimal water resources systems analysis. in (Prentice Hall, 1989).
10. Rio, P. C. *et al.* Water Resources Optimization Method in the Context of Climate Change. *Article in Journal of Water Resources Planning and Management* (2015) doi:10.1061/(ASCE)WR.1943-5452.0000445.
11. Dias, N. L. C., Pereira, M. V. F. & Kelman, J. Optimization of Flood Control and Power Generation Requirements in a Multi-Purpose Reservoir. *IFAC Proceedings Volumes* **18**, 101–104 (1985).
12. Kelman, J., Cooper, L. A., Hsu, E. & Yuan, S.-Q. Use of probabilistic constraints in reservoir operation policies with sampling stochastic dynamic programming. in *Computerized Decision Support Systems for Water Managers* 508–515 (ASCE, 1988).
13. Anghileri, D. *et al.* Optimizing Watershed Management by Coordinated Operation of Storing Facilities Trading off sediment connectivity and energy production through network scale optimization of hydropower portfolios View project Optimizing Watershed Management by Coordinated Operation of Storing Facilities. *Article in Journal of Water Resources Planning and Management* (2013) doi:10.1061/(ASCE)WR.1943-5452.0000313.
14. Chen, C., Yuan, Y. & Yuan, X. An Improved NSGA-III Algorithm for Reservoir Flood Control Operation. *Water Resources Management* **31**, 4469–4483 (2017).

15. Davidsen, C. ; *et al.* Using Stochastic Dynamic Programming to Support Water Resources Management in the Ziya River Basin. *China. Journal of Water Resources Planning and Management* **141**, (2015).
16. Delipetrev, B., Jonoski, A. & Solomatine, D. P. A novel nested dynamic programming (nDP) algorithm for multipurpose reservoir optimization. *Journal of Hydroinformatics* **17**, 570–583 (2015).
17. Mabaya, G., Unami, K. & Fujihara, M. Stochastic optimal control of agrochemical pollutant loads in reservoirs for irrigation. *J Clean Prod* **146**, 37–46 (2017).
18. Turner, S. W. D. & Galelli, S. Regime-shifting streamflow processes: Implications for water supply reservoir operations. *Water Resour Res* **52**, 3984–4002 (2016).
19. Tsitsiklis, J. N. & van Roy, B. Feature-Based Methods for Large Scale Dynamic Programming. *Machine Learning 1996 22:1* **22**, 59–94 (1996).
20. Powell, W. B. *Approximate Dynamic Programming: Solving the curses of dimensionality*. vol. 703 (John Wiley & Sons, 2007).
21. Reed, P. M. & Kollat, J. B. Visual analytics clarify the scalability and effectiveness of massively parallel many-objective optimization: A groundwater monitoring design example. *Adv Water Resour* **56**, 1–13 (2013).
22. Giuliani, M., Galelli, S. & Soncini-Sessa, R. A dimensionality reduction approach for many-objective Markov Decision Processes: Application to a water reservoir operation problem. *Environmental Modelling & Software* **57**, 101–114 (2014).
23. Bertsekas, D. *Reinforcement learning and optimal control*. (Athena Scientific, 2019).
24. Powell, W. B. A unified framework for stochastic optimization. *Eur J Oper Res* **275**, 795–821 (2019).
25. Bertsekas, D. P. Dynamic Programming and Suboptimal Control: A Survey from ADP to MPC*. *Eur J Control* **11**, 310–334 (2005).
26. Deisenroth, M. & Rasmussen, C. E. PILCO: A model-based and data-efficient approach to policy search. in *Proceedings of the 28th International Conference on machine learning (ICML-11)* 465–472 (Citeseer, 2011).
27. Giuliani, M., Lamontagne, J. R., Reed, P. M. & Castelletti, A. A State-of-the-Art Review of Optimal Reservoir Control for Managing Conflicting Demands in a Changing World. *Water Resour Res* **57**, e2021WR029927 (2021).
28. Giuliani, M. *et al.* Participatory design of robust and sustainable development pathways in the Omo-Turkana river basin. *J Hydrol Reg Stud* **41**, 101116 (2022).
29. Bertoni, F., Castelletti, A., Giuliani, M. & Reed, P. M. Discovering Dependencies, Trade-Offs, and Robustness in Joint Dam Design and Operation: An Ex-Post Assessment of the Kariba Dam. *Earths Future* **7**, 1367–1390 (2019).
30. Giudici, F., Castelletti, A., Garofalo, E., Giuliani, M. & Maier, H. R. Dynamic, multi-objective optimal design and operation of water-energy systems for small, off-grid islands. *Appl Energy* **250**, 605–616 (2019).

31. Baxter, J. & Bartlett, P. L. Infinite-horizon policy-gradient estimation. *Journal of Artificial Intelligence Research* **15**, 319–350 (2001).
32. Denaro, S., Anghileri, D. & Giuliani, M. Informing the operations of water reservoirs over multiple temporal scales by direct use of hydro-meteorological data. (2017).
33. Giuliani, M., Herman, J. D., Castelletti, A. & Reed, P. Many-objective reservoir policy identification and refinement to reduce policy inertia and myopia in water management. *Water Resour Res* **50**, 3355–3377 (2014).
34. Tikk, D., Kóczy, L. T. & Gedeon, T. D. A survey on universal approximation and its limits in soft computing techniques. *International Journal of Approximate Reasoning* **33**, 185–202 (2003).
35. Zoppoli, R., Sanguineti, M. & Parisini, T. Approximating networks and extended Ritz method for the solution of functional optimization problems. *J Optim Theory Appl* **112**, 403–440 (2002).
36. Cybenko, G. Approximation by superpositions of a sigmoidal function. *Mathematics of Control, Signals, and Systems (MCSS)* **2**, 303–314 (1989).
37. Funahashi, K.-I. On the approximate realization of continuous mappings by neural networks. *Neural networks* **2**, 183–192 (1989).
38. Chen, T. & Chen, H. Universal approximation to nonlinear operators by neural networks with arbitrary activation functions and its application to dynamical systems. *IEEE Trans Neural Netw* **6**, 911–917 (1995).
39. Giuliani, M., Quinn, J. D., Herman, J. D., Castelletti, A. & Reed, P. M. Scalable Multiobjective Control for Large-Scale Water Resources Systems under Uncertainty. *IEEE Transactions on Control Systems Technology* **26**, 1492–1499 (2018).
40. Coello, C. A. C., Lamont, G. B. & Veldhuizen, D. A. Van. *Evolutionary Algorithms for Solving Multi-Objective Problems*. *Evolutionary Algorithms for Solving Multi-Objective Problems* (Springer US, 2007). doi:10.1007/978-0-387-36797-2.
41. Maier, H. R. *et al.* Evolutionary algorithms and other metaheuristics in water resources: Current status, research challenges and future directions. *Environmental Modelling & Software* **62**, 271–299 (2014).
42. Busa-Fekete, R., Szörényi, B., Weng, P., Cheng, W. & Hüllermeier, E. Preference-based reinforcement learning: evolutionary direct policy search using a preference-based racing algorithm. *Mach Learn* **97**, 327–351 (2014).
43. Zatarain Salazar, J., Reed, P. M., Herman, J. D., Giuliani, M. & Castelletti, A. A diagnostic assessment of evolutionary algorithms for multi-objective surface water reservoir control. *Adv Water Resour* **92**, 172–185 (2016).
44. Hadka, D. & Reed, P. Borg: An auto-adaptive many-objective evolutionary computing framework. *Evol Comput* **21**, 231–259 (2013).
45. Reed, P. M., Hadka, D., Herman, J. D., Kasprzyk, J. R. & Kollat, J. B. Evolutionary multiobjective optimization in water resources: The past, present, and future. *Adv Water Resour* **51**, 438–456 (2013).
46. Georgakakos, A. P. & Yo, H. *A decision support tool for the Nile basin*. (2003).

47. CAPMAS(2019), SECTION (5) LAND RECLAMATION & AGRICULTURE.
48. Ministery of water resources and Irrigation. *National Water Resources Plan 2017*. (2005).
49. El-Essawy, H., Nasr, P. & Sewilam, H. Aquaponics: a sustainable alternative to conventional agriculture in Egypt – a pilot scale investigation. *Environmental Science and Pollution Research* **26**, 15872–15883 (2019).
50. Turnšek, M. *et al.* Commercial aquaponics: a long road ahead. *Aquaponics food production systems* **18**, 453–485 (2019).
51. Nelson, R. L. & Pade, J. S. Aquaponic food production: growing fish and vegetables for food and profit. (2008).
52. Wittholz, M. K., O'Neill, B. K., Colby, C. B. & Lewis, D. Estimating the cost of desalination plants using a cost database. *Desalination* **229**, 10–20 (2008).
53. Al-Nory, M. & El-Beltagy, M. An energy management approach for renewable energy integration with power generation and water desalination. *Renew Energy* **72**, 377–385 (2014).
54. Kaya, A., Evren Tok, M. & Koc, M. A Levelized Cost Analysis for Solar-Energy-Powered Sea Water Desalination in The Emirate of Abu Dhabi. *Sustainability 2019, Vol. 11, Page 1691* **11**, 1691 (2019).
55. Karagiannis, I. C. & Soldatos, P. G. Water desalination cost literature: review and assessment. *Desalination* **223**, 448–456 (2008).
56. Sandoval-Solis, S., McKinney, D. C. & Loucks, D. P. Sustainability index for water resources planning and management. *J Water Resour Plan Manag* **137**, 381–390 (2011).
57. Progress on level of water stress. doi:10.4060/cb6241en.
58. Indicator | SDG 6 Data. https://sdg6data.org/indicator/6.5.2.